Siderophore specificities of the Pseudomonas aeruginosa TonB-dependent transporters ChtA and ActA

Virginie Will, Véronique Gasser, Lauriane Kuhn, Sarah Fritsch, David Heinrichs, Isabelle Schalk

FEBS Letters

FEBS PR
science publishing b

Siderophore specifities of ChtA and ActA, two TonB-dependent transporters of *Pseudomonas aeruginosa*

Journal:	*FEBS Letters*
Manuscript ID	FEBSL-23-0596.R1
Wiley - Manuscript type:	Research Article
Date Submitted by the Author:	n/a
Complete List of Authors:	Will, Virginie; University of Strasbourg; CNRS Gasser, Véronique; University of Strasbourg; CNRS Kuhn, Lauriane; University of Strasbourg; CNRS Fritsch, Sarah; University of Strasbourg; CNRS Heinrichs, David; University of Western Ontario, Microbiology and Immunology Schalk, Isabelle; University of Strasbourg, UMR7242; CNRS, UMR7243
Keywords:	Siderophore, iron homeostasis, Pseudomonas aeruginosa, outer membrane transporters
Abstract:	Iron is an essential nutrient for the pathogen *Pseudomonas aeruginosa*. To access iron, the pathogen is able to express at least 15 different iron-uptake pathways, the vast majority involving small iron chelators called siderophores. *P. aeruginosa* produces two siderophores, but can also use many produced by other microorganisms. This implies that the bacterium expresses appropriate TonB-dependent transporters (TBDTs) at the outer membrane to import the ferric form of each of the siderophores used. Here, we show that the two α-carboxylate type siderophores rhizoferrin-Fe and staphyloferrin A-Fe are transported into *P. aeruginosa* cells by the TBDT ActA. Among the mixed α-carboxylate/hydroxamate type siderophores, we found aerobactin-Fe to be transported by ChtA and schizokinen-Fe and arthrobactin-Fe by ChtA and another unidentified TBDT.

Siderophore specifities of ChtA and ActA, two TonB-dependent transporters of *Pseudomonas aeruginosa*

Virginie Will[1,2], Véronique Gasser[1,2], Lauriane Kuhn[3], Sarah Fritsch[1,2], David E. Heinrichs[4] and Isabelle J. Schalk[1,2 *].

[1] CNRS, University of Strasbourg, UMR7242, UMR7242, ESBS, Bld Sébastien Brant, F-67412 Illkirch, Strasbourg, France

[2] University of Strasbourg, UMR7242, ESBS, Bld Sébastien Brant, F-67412 Illkirch, Strasbourg, France

[3] Plateforme Proteomique Strasbourg - Esplanade, Institut de Biologie Moléculaire et Cellulaire, CNRS, FR1589, 15 rue Descartes, F-67084 Strasbourg Cedex, France

[4]Department of Microbiology and Immunology, University of Western Ontario, London, Ontario, CANADA N6A 5C1

[*] To whom correspondence should be addressed: isabelle.schalk@unistra.fr

ABSTRACT

Iron is an essential nutrient for the pathogen *Pseudomonas aeruginosa*. To access iron, the pathogen is able to express at least 15 different iron-uptake pathways, the vast majority involving small iron chelators called siderophores. *P. aeruginosa* produces two siderophores, but can also use many produced by other microorganisms. This implies that the bacterium expresses appropriate TonB-dependent transporters (TBDTs) at the outer membrane to import the ferric form of each of the siderophores used. Here, we show that the two α-carboxylate type siderophores rhizoferrin-Fe and staphyloferrin A-Fe are transported into *P. aeruginosa* cells by the TBDT ActA. Among the mixed α-carboxylate/hydroxamate type siderophores, we found aerobactin-Fe to be transported by ChtA and schizokinen-Fe and arthrobactin-Fe by ChtA and another unidentified TBDT.

INTRODUCTION

Iron is an essential nutrient for the growth and virulence of *P. aeruginosa*, a ubiquitous bacterium and opportunistic pathogen often responsible for lung infections. *P. aeruginosa* is able to express and use at least 15 different iron acquisition pathways, each involving a specific set of proteins [1]. Among these import pathways, three involve different heme import strategies [2,3], one uses ferrous iron [4], and a large range use siderophores [1]. Siderophores are small molecules with a molecular mass between 200 and 2000 Da characterized by a very strong affinity for ferric iron [5]. They show an enormous diversity in their chemical structure, with certain siderophores exclusively possessing catecholate, hydroxamate, or α-hydroxy-carboxylate residues for iron chelation, and many others exhibiting mixtures of different chelating functions [5].

Siderophores are synthesized by bacteria, fungi and plants and secreted into their environment to access iron. For Gram-negative bacteria, once siderophores have scavenged iron, their ferric complexes are transported back through the outer membrane by TonB-dependent transporters (TBDT) [6]. The uptake activity of TBDTs is dependent on a molecular motor, located in the inner membrane, composed of the three proteins: TonB, ExbB, and ExbD [7–10]. The structure of TBDTs is characterized by a β barrel, allowing insertion into the outer membrane, and a globular or plug domain that closes the lumen of the barrel [6]. A binding site is located on the extracellular side of the plug domain and is able to specifically recognize an iron-charged siderophore or a set of ferri-siderophores of very close chemical structure. The TonB-ExbB-ExbD protein complex is activated by the proton gradient through the inner membrane. As a consequence, the TonB protein interacts with the N-terminal periplasmic domain of the TBDTs to allow formation of a channel through the transporter and the import of ferri-siderophore complexes [7–10]. Depending on the pathway, the iron dissociates from the siderophore, either in the periplasm or cytoplasm, with transport of the ferri-siderophore complexes through the inner membrane via specific transporters in the second case [11].

P. aeruginosa produces two siderophores, pyoverdine and pyochelin [12], and can use many siderophores produced by other microorganisms (xenosiderophores) [1]. The ability of *P. aeruginosa* to use siderophores produced by other bacteria is due to the presence of numerous genes encoding TBDTs in its genome, each recognizing and importing a different iron-loaded xenosiderophore or a family of xenosiderophores of similar structure. The xenosiderophores that can be used by *P. aeruginosa* include mycobactins and carboxymycobactins (with FemA as the TBDT, [13]), enterobactin (PfeA and PirA for the TBDTs involved, [14,15]), vibriobactin (FvbA, [16]), nocardamine (FoxA, [17]), ferrichrome and ferrioxamine B (FiuA and FpvB, [18–20]), and even citrate (FecA, [21]). Recently, it has also been demonstrated that monocatechols, such as catecholamine neuro-mediators or plant derived catechols can be used as siderophores by *P. aeruginosa,* with PiuA and PirA as the TBDTs involved [22,23].

Here, we investigated the ability of *P. aeruginosa* to use two α-carboxylate type siderophores, rhizoferrin (RHIZOF) and staphyloferrin A (STAPH A), and revisited the ability to use mixed α-carboxylate/hydroxamate siderophores, aerobactin (AERO), arthrobactin (ARTHRO) and schizokinen (SCHIZO). RHIZOF is produced by Zygomycetes, such as *Mucor lusitanicus* [24], STAPH A by *Staphylococcus aureus* and many members of the coagulase-negative staphylococci [25]), AERO by *E. coli* and hypervirulent *Klebsiella pneumoniae* strains [26], ARTHRO by *Arthrobacter pascens* ATCC 13346 [27], and SCHIZO by *Rhizobium* and *Bacillus megaterium* [28,29] (Figure 1). Previous studies had shown that AERO, SCHIZO and rhizobactin (a siderophore of the same family as RHIZOF) use the TBDT ChtA to import iron into *P. aeruginosa* cells [30]. As we had no access to rhizobactin, we tested here only RHIZOF (rhizoferrin). Here using ^{55}Fe uptake and growth assays, we show that the TBDTs involved are: ActA (α-carboxylate transporter A, gene PA3268) for RHIZOF and STAPH A, ChtA for AERO, and ChtA and another unidentified TBDT for SCHIZO and ARTHRO.

MATERIALS AND METHODS

Chemicals. RHIZOF, AERO, ARTHRO and SCHIZO were purchased from EMC Microcollections (Tübingen, Germany), and STAPH A was synthesized as previously described [31]. The protonophore carbonyl cyanide m-chlorophenylhydrazone (CCCP) was purchased from Sigma-Aldrich and $^{55}FeCl_3$ was purchased from Perkin Elmer.

Bacterial strains, plasmids, and growth conditions. The *P. aeruginosa* strains used in this study are listed in Table S1 in Supplemental Materials. The iron-deficient CAA (casamino acid) medium used is composed of 5g l^{-1} low-iron CAA (Difco), 1.46 g l^{-1} K_2HPO_4 $3H_2O$, and 0.25 g l^{-1} $MgSO_4$ $7H_2O$.

Plasmid and strain construction. Enzymes were obtained from ThermoFisher Scientific. *Escherichia coli* TOP10 (Invitrogen) was used as the host strain for the plasmids. Plasmid construction and mutagenesis in the chromosomal genome of *P. aeruginosa* were performed as previously described [32]. Briefly, the blunt-end ligation strategy was used to insert 1400 bp of flanking sequences of the genes *chtA* or *actA* into the suicide vector pEXG2. The plasmids were then sequenced and used to introduce chromosomal mutations into the *P. aeruginosa* Δ*pvdF*Δ*pchA* strain. All generated mutants were verified by PCR and sequencing.

Iron uptake. Xenosiderophore-^{55}Fe complexes were prepared at ^{55}Fe concentrations of 50 µM, with a xenosiderophore:iron (mol:mol) ratio of 20:1, as described previously. *P. aeruginosa* strains were successively grown overnight in LB broth, followed by overnight growth in CAA medium and, finally, overnight growth in CAA medium with either 10 µM RHIZOF, STAPH A, AERO, ARTHRO or SCHIZO, all at 30°C. The bacteria were subsequently used to study ^{55}Fe uptake kinetics, as described previously, in the presence or absence of 200 µM CCCP (a proton motive force inhibitor) at a concentration of xenosiderophore-^{55}Fe complexes of 500 nM, with a xenosiderophore:iron (mol:mol) ratio of 20:1 [33,34].

Growth assays in iron-restricted conditions. For *P. aeruginosa* growth assays in microplates, bacteria were grown as described above: a first overnight culture at 30°C in 5 mL LB broth, followed by washing of the bacteria and a second overnight culture in 10 mL CAA medium at 30°C. Bacteria were then washed, resuspended in CAA medium at an optical density of 0.01 at 600 nm, and distributed in the wells of a 96-well plate (Greiner, U-bottom microplate) in the presence or absence of 10 µM RHIZOF, STAPH A, AERO, ARTHRO or SCHIZO. The plate was incubated at 30°C, with shaking, in a TECAN microplate reader (Infinite M200, Tecan) and bacterial growth monitored at $OD_{600\ nm}$. The presented data are the mean of three replicates for each measurement.

Proteomic analysis. *P. aeruginosa* Δ*pvdF*Δ*pchA* cells were consecutively grown overnight in LB and then CAA medium. Bacteria were then pelleted and diluted again in CAA medium at an $OD_{600\ nm}$ of 0.1 and grown for 8 h with or without 10 µM xenosiderophores at 30°C. The cells (5×10^8) were harvested and used for proteomic analysis. A biological triplicate was prepared for each sample for each cell-culture condition. Cell pellets were resuspended in 200 µL lysis buffer (UTCT buffer containing 7 M urea, 2 M thiourea, 4% CHAPS, and 20 mM Tris-HCl pH 7.6) supplemented with nuclease and DNase. Protein concentrations were determined with the Bradford assay using bovine serum albumin as the standard. Proteins were further precipitated overnight with glacial 0.1 M ammonium acetate in 100% methanol (5 volumes, -20°C). After centrifugation at 12,000 x g and 4°C for 15 min, the resulting pellets were washed twice with 0.1 M ammonium acetate in 80% methanol and further dried under vacuum (Speed-Vac concentrator). Pellets were resuspended in 100 µL 50 mM ammonium bicarbonate and reduced (5 mM dithiothreitol, 95°C, 10 min) and alkylated (10 mM iodoacetamide, room temperature, 20 min). Proteins were finally digested overnight with 150 ng sequencing-grade trypsin (Promega). The proteomic data sets were obtained by injecting 1000 ng of each peptide mixture into a TripleTOF 5600 mass spectrometer (Sciex) coupled to an U3000-RSLC

liquid chromatography (Thermo-Fisher Scientific), as described previously. For both differential proteomic analyses, data were searched against the *P. aeruginosa* UniprotKB sub-database (UniprotKB release 2016_12, taxon 208964, *P. aeruginosa* strain PAO1, 5564 forward protein sequences). Peptides and proteins were identified using the Mascot algorithm (version 2.5.1, Matrix Science, London, UK). The following parameters were used: (i) Trypsin/P was selected as the enzyme, (ii) two missed cleavages were allowed, (iii) methionine oxidation and acetylation of the protein N-terminus were set as variable modifications and carbamidomethylation of cysteine as a fixed modification, (iv) mass tolerance for precursor ions was set to 10 ppm and 0.02 Da for fragment ions. Mascot data were further imported into Proline v1.4 software [35]. Proteins were validated against a Mascot pretty rank equal to 1 and a 1% FDR for both peptide spectrum matches (PSM score) and protein sets (Protein Set score). All MS/MS fragmentation spectra were used to quantify each protein from at least three independent biological replicates: this “BasicSC” value, calculated by Proline, included all PSMs of all peptides, including modified peptides (3 fixed and variable modifications) and the peptides shared by different protein sets. After column-wise normalization of the data matrix, the “BasicSC” spectral count values were subjected to a negative-binomial test using edgeR GLM regression of R (R v3.2.5) through the IPinquiry package [36]. The statistical test was based on the published msmsTests R package available in Bioconductor to process label-free LC-MS/MS data by spectral counts [37]. For each identified protein, an adjusted P-value (adjp), corrected by the Benjamini–Hochberg procedure, was calculated, as well as the protein fold-change (FC). The MS data were deposited in the ProteomeXchange Consortium database via the PRIDE [38] partner repository with the dataset identifier PXD043056 and 10.6019/PXD043056 (Reviewer account details: Username: reviewer_pxd043056@ebi.ac.uk, Password: Ev8yglfz).

Quantitative real-time PCR. The expression of specific genes of interest was monitored by quantitative reverse transcription PCR (qRT-PCR) as described previously [32,39]. After a first overnight incubation in LB medium, Δ*pvdF*Δ*pchA* cells were grown in 10 mL CAA medium. Bacteria were then washed, resuspended in CAA medium at an optical density of 0.1 at 600 nm, and incubated in the presence of 10 or 100 µM RHIZOF, STAPH A, AERO, ARTHRO or SCHIZO, with shaking (220 rpm), at 30°C. After 8 h of incubation, 2.5 X 10^8 cells were collected from the cultures and two volumes of RNAprotect Bacteria Reagent (Qiagen) was added. Total RNA was extracted from the pellet using the RNeasy Plus Mini Kit (Qiagen) following the manufacturer instructions. Total RNA (1 µg) was reverse transcribed using the iScript cDNA Synthesis Kit (Biorad). Specific cDNA in our samples was quantified using a CFX Opus 96 (Biorad), the appropriate primers (Table S3), and iTaq Universal SYBR Green Supermix (Biorad). The transcript level for each gene was normalized against those of *uvrD* and *rpsI* and are expressed as a log2 ratio (fold-change) relative to the reference condition.

RESULTS AND DISCUSSION

RHIZOF, STAPH A, AERO, ARTHRO and SCHIZO transport ^{55}Fe into* P. aeruginosa *cells. We investigated the ability of AERO, ARTHRO, SCHIZO, RHIZOF, and STAPH A to be used as xenosiderophores by *P. aeruginosa* and compared their efficiency of iron uptake by using ^{55}Fe. *P. aeruginosa* Δ*pvdF*Δ*pchA* (Table S1 in Supplemental Materials), a strain unable to produce the siderophores PVD and PCH, was grown under iron-starvation conditions and in the presence of 10 µM of the apo form (without iron) of one of the xenosiderophores to induce expression of the corresponding iron-uptake pathway. Indeed, previous studies have shown that *P. aeruginosa* is able to detect the presence of certain xenosiderophores in its environment and induce expression of the proteins belonging to the corresponding iron-uptake pathway in response [13,18,32,39–42]. The Δ*pvdF*Δ*pchA* mutant was used to avoid any iron uptake by the siderophores pyoverdine and pyochelin produced by *P. aeruginosa*. Δ*pvdF*Δ*pchA* cells were then incubated in the presence of one of the five xenosiderophores in complex with ^{55}Fe and the radioactivity incorporated into the bacteria followed as a function of time. We observed ^{55}Fe accumulation for RHIZOF, STAPH A, AERO and SCHIZO , with very similar uptake rates of approximately 280-400 pmol.mL^{-1}.OD$_{600\ nm}^{-1}$ after a 3 h incubation (Figure 2A, B, C and E, kinetics in green). This is within the range that has been previously reported for pyoverdine and pyochelin [32,43,44]. The ^{55}Fe uptake rates for ARTHRO was clearly less efficient (Figure 2D, kinetic in green). ^{55}Fe accumulation was no longer observed for Δ*pvdF*Δ*pchA* cells pre-incubated with the protonophore CCCP for all five xenosiderophores (kinetics in yellow), demonstrating that the iron uptake observed for these compounds is dependent on the bacterial proton motive force. Therefore, the observed ^{55}Fe uptake was not due to passive diffusion across the outer membrane via porins or non-specific association with the cell surface, but rather to transport carried out by TBDTs. In conclusion, the five xenosiderophores RHIZOF, STAPH A, AERO, ARTHRO and SCHIZO, can transport iron into *P. aeruginosa* cells and act as xenosiderophores, but this uptake is clearly less efficient for ARTHRO

None of these xenosiderophores significantly induces the transcription or expression of a TBDT. Previous studies have shown that the presence of certain xenosiderophores, such as enterobactin, nocardamine, or ferrichrome, in the environment of *P. aeruginosa* induces the expression of the corresponding TBDT by mechanisms involving sigma/anti-sigma factors, two-component systems, or AraC type transcriptional regulators [32,42]. Such induction of expression of the TBDT corresponding by its xenosiderophore often goes hand to hand with repression of the expression of the genes involved in the uptake of iron by pyochelin, whereas no effect is generally seen for the genes involved in iron uptake by pyoverdine [17,32,39,42,43].

Proteomic analyses of *P. aeruginosa* Δ*pvdF*Δ*pchA* grown in the presence or absence of 10 µM of RHIZOF, STAPH A, AERO and SCHIZO, showed the induction of *chtA* and *actA* (*PA3268*) expression, with fold changes between 1.87 and 5.2, but with poor statistics suggesting that the expression induction observed may be an artefact (Figure S1, ARTHRO was not tested since the ^{55}Fe uptake was low). Indeed, such induction of *chtA* and *actA* expression was not confirmed at the transcriptional level by qRT-PCR (Figure S2). For the qRT-PCR assay, we tested two concentrations of xenosiderophores, 10 and 100 µM, expecting that the transcription of *chtA* and/or *actA* could be induced by the higher concentration of xenosiderophores. The effect of ARTHRO on *chtA* and/or *actA* transcription was also tested in qRT-PCR. We observed no induction of the transcription of these two genes, even at 100 µM for all five xenosiderophores indicating these xenosiderophores are not able to induce the transcription and expression of *chtA* or *actA* when present in the environment of *P. aeruginosa*. ChtA has been previously reported to be involved in the uptake of iron via AERO, SCHIZO, and rhizobactin [30]. ActA is encoded by the gene PA3268, but the ligand transported by this transporter has not yet been identified. Surprisingly, *oprC* expression was repressed in the presence of 10 µM RHIZOF, SCHIZO, or STAPH A, with fold changes between -5.6 and -2.5 relative to cells grown in the absence of any xenosiderophore (Figure S1). OprC is a TBDT involved in copper acquisition [45]. Such a reduction in *oprC* expression could not be confirmed at the transcriptional level by qRT-PCR (Figure S2), raising

doubts about its biological significance and the possibility that these xenosiderophores may import copper.

In conclusion, the proteomic and qRT-PCR data were not consistent concerning the induction of transcription and expression of *chtA* and *actA* by RHIZOF, STAPH A, AERO, ARTHRO or SCHIZO, making it difficult to draw any definitive conclusions. If expression of one of these TBDTs is induced by one of the xenosiderophores tested, it may be at a low level that is not easily detected by the approaches used here.

ActA imports iron via RHIZOF and STAPH A, the two α-carboxylate type xenosiderophores. We further investigated the uptake pathway used by RHIZOF and STAPH A to import iron using a growth assay described previously [44] with the Δ*pvdF*Δ*pchA* strain grown under iron-restricted conditions (CAA medium containing approximately 20 nM iron, [46]). In this growth condition, the *P. aeruginosa* strain is unable to produce pyoverdine and pyochelin and probably accesses iron via citrate or imports ferrous iron after reduction. Addition of 10 µM RHIZOF or STAPH A to this medium stimulated growth for both xenosiderophores tested, confirming that they can promote Δ*pvdF*Δ*pchA* growth by importing iron into the bacteria (Figure 3). In this assay, the presence of a xenosiderophore unable to import iron into *P. aeruginosa* cells completely inhibited growth, as previously shown for bacillibactin [44].

We used both the growth and ^{55}Fe uptake assays to try to identify the TBDTs involved in the uptake of iron by these xenosiderophores. If a TBDT is involved, deletion of its gene should affect the growth of the bacteria, because no more iron uptake occurs. In the presence of RHIZOF and STAPH A, complete growth inhibition was observed when *actA* (*PA3268*) was deleted, clearly showing that ActA is the only TBDT that imports iron via these two xenosiderophores (Figure 3). Mutation of *chtA* had no effect on growth in the presence of RHIZOF, indicating that unlike rhizobactin [30], ChtA is not involved in iron acquisition by RHIZOF. Concerning the ^{55}Fe assay, surprisingly, mutation of *actA* did not completely

abolish ^{55}Fe uptake for either the RHIZOF-^{55}Fe or STAPH A-^{55}Fe complexes (69% and 39% inhibition, respectively, Figure 2), contrary to what would have been expected from the results of the growth experiments, and mutation of *chtA* had no effect on ^{55}Fe import. The remaining ^{55}Fe uptake observed for the Δ*pvdF*Δ*pchA*Δ*actA* strain likely corresponds to the uptake of RHIZOF-^{55}Fe and STAPH-^{55}Fe via another pathway involving an unidentified TBDT. However, iron taken up via this uptake pathway appears to not be bioavailable for *P. aeruginosa*, as deletion of *actA* alone completely abolished growth in iron-restricted medium (Figure 3). One explanation could be that iron cannot be removed from RHIZOF and STAPH A in this second unidentified uptake pathway because it is unable to interact with the enzyme(s) involved in this process. Another possibility is that ^{55}Fe in this second uptake pathway is blocked in the periplasm and unable to reach the cytoplasm because the two xenosiderophore-^{55}Fe complexes are unable to be transported across the inner membrane.

Overall, these data show that ActA is the TBDT of the α-carboxylate type siderophores RHIZOF and STAPH A. Another TBDT is apparently also able to import the two RHIZOF-^{55}Fe and STAPH-^{55}Fe complexes across the outer membrane, but the iron is not bioavailable for *P. aeruginosa* cells. Contrary to what has been reported previously for rhizobactin [30], ChtA is not involved in iron acquisition by RHIZOF, which is surprising since both xenosiderophores have close chemical structures. It would be interesting to revisit the ability of ChtA to import iron via rhizobactin (unfortunately we were unable to get purified rhizobactin).

ChtA is the TBDT involved in the uptake of iron by AERO, ARTHRO, and SCHIZO, the three mixed α-carboxylate/hydroxamate type xenosiderophores. Using the same strategy as described above, we observed complete inhibition of bacterial growth in the presence of AERO when the *chtA* gene was deleted, indicating that ferri-AERO is transported into *P. aeruginosa* cells exclusively by this TBDT (Figure 4). In the presence of ARTHRO or SCHIZO, the growth of Δ*pvdF*Δ*pchA*Δ*chtA* was only partially (54 and 45% respectively) affected by deletion of *chtA* compared to the growth of Δ*pvdF*Δ*pchA*.

Deletion of *actA* had no additional inhibitory effect on the growth of the Δ*pvdF*Δ*pchA*Δ*chtA*Δ*actA* *mutant*. As complete inhibition of growth was not observed with deletion of either *chtA* or *actA*, at least one other unidentified TBDT is involved in the uptake of iron by ARTHRO and SCHIZO. Concerning the ^{55}Fe assay, the deletion of *chtA* completely abolished the import of iron by AERO, perfectly consistent with the results observed in the growth experiment, confirming that ChtA is the only TBDT involved in iron import by this xenosiderophore. For ARTHRO and SCHIZO, the deletion of *actA* had no effect on ^{55}Fe uptake, and the deletion *chtA* abolished 51 and 81% of ^{55}Fe uptake respectively, a greater impact than that observed on bacterial growth. One explanation could be that the second unidentified TBDT involved is less efficient in importing iron but still allows the bacteria to survive in an iron-restricted environment. Such lower efficiency could come from lower expression of the TBDT involved or lower affinity of the Ferri-ARTHRO and ferri-SCHIZO complexes for the binding site of this TBDT.

Overall, these data show that ChtA transports the ferri forms of the mixed α-carboxylate/hydroxamate siderophores AERO, ARTHRO and SCHIZO, confirming previous studies [30]. However, according to our data, another unidentified transporter is also involved in ferri-ARTHRO and ferri-SCHIZO transport.

CONCLUSION

Here, we show that *P. aeruginosa* can use RHIZOF, STAPH A, AERO, ARTHRO and SCHIZO as siderophores, expanding the number of xenosiderophores used by this pathogen. RHIZOF, STAPH A, AERO, and SCHIZO transport ^{55}Fe with an efficiency close to that previously reported for pyoverdine, pyochelin, enterobactin, ferrichrome, and nocardamine [17,32]. ^{55}Fe uptake by ARTHRO was less efficient. The fact that this bacterium can use many xenosiderophores is an advantage for its survival in various microbial communities. For example, *S. aureus* and *P. aeruginosa* are frequently co-isolated from chronic infection, including the pulmonary infections of persons with cystic fibrosis (CF) and chronic wounds [47–51]. The ability of *P. aeruginosa* to use STAPH A to access iron may play a key role

in such co-infections. Recent studies have also shown that *S. aureus* inactivates *P. aeruginosa* siderophore pyochelin via methylation, indicating as well that competition for iron must be a though battle between both pathogens in co-infections [52]. The two α-carboxylate type xenosiderophores, RHIZOF-Fe and STAPH A-Fe, are transported into *P. aeruginosa* cells by ActA (*PA3268*), a TBDT for which the transported molecule had not been identified to date (Scheme 1). The gene *PA3269*, encoding an AraC type transcriptional regulator, is localized next to the *actA* gene, suggesting that *actA* transcription should involve a molecular mechanism similar to that of *fptA* (ferri-pyochelin TBDT). Indeed, PchR is a AraC transcriptional regulator capable to bind ferri-pyochelin transported into the bacteria by FptA, and inducing the transcription of *fptA* [41,53,54]. According the transcriptomic and proteomic data presented above, RHIZOF and STAPH A appear to be unable to efficiently induce *actA* transcription and expression.

For the mixed α-carboxylate/hydroxamate type xenosiderophores, AERO-Fe is transported by ChtA (as previously described [30]) and ARTHRO-Fe and SCHIZO-Fe, by ChtA and another unidentified TBDT (Scheme 1). These two TBDTs, ActA and ChtA, have different binding selectivity: ActA is specific for α-carboxylate type siderophores and ChtA for mixed α-carboxylate/hydroxamate siderophores.

ACKNOWLEDGMENTS

Authors acknowledge the Centre National de la Recherche Scientifique (CNRS) for general financial support. The presented work was also supported by a grant from the CNRS (80/Prime 2020), as well as with a grant from the Agence Nationale de la Recherche (ANR, grant number: ANR-22-CE44-0024-01). We also acknowledge the Interdisciplinary Thematic Institute (ITI) InnoVec (Innovative Vectorization of Biomolecules, IdEx, ANR-10-IDEX-0002). The mass spectrometry instrumentation at the IBMC was funded by the University of Strasbourg, IdEx "Equipement mi-lourd" 2015. VW had a fellowship from the Ministry of Research and

Education. Work in the Heinrichs laboratory was funded by Canadian Institutes of Health Research grant PJT-183848.

AUTHORS CONTRIBUTIONS

VW carried out all the ^{55}Fe uptake assays, qRT-PCR, and bacterial growth assays, and prepared the figures of the manuscript; LK: carried out the proteomic experiments and analyses, writing – review & editing; SF: generated the mutants used in the manuscript; DEH: provided the staphyloferrin; GV: Conceptualization, supervised the biological experiments; IJS: Conceptualization, supervised the biological experiments, writing – review & editing, funding acquisition, project administration. All authors reviewed the manuscript.

REFERENCES

1 Schalk IJ & Perraud Q (2023) *Pseudomonas aeruginosa* and its multiple strategies to access iron. *Environ Microbiol*. **25**, 811-831

2 Smith AD & Wilks A (2015) Differential contributions of the outer membrane receptors PhuR and HasR to heme acquisition in *Pseudomonas aeruginosa*. *J Biol Chem* **290**, 7756–7766.

3 Otero-Asman JR, García-García AI, Civantos C, Quesada JM & Llamas MA (2019) *Pseudomonas aeruginosa* possesses three distinct systems for sensing and using the host molecule haem. *Environ Microbiol*. **21**, 4629-4647

4 Lau CKY, Krewulak KD & Vogel HJ (2016) Bacterial ferrous iron transport: the Feo system. *FEMS Microbiol Rev.* **40**, 273–298.

5 Hider RC & Kong X (2011) Chemistry and biology of siderophores. *Nat Prod Rep* **27**, 637–57.

6 Schalk IJ, Mislin GLA & Brillet K (2012) Structure, function and binding selectivity and stereoselectivity of siderophore-iron outer membrane transporters. *Curr Top Membr* **69**, 37–66.

7 Celia H, Noinaj N, Zakharov SD, Bordignon E, Botos I, Santamaria M, Barnard TJ, Cramer WA, Lloubes R & Buchanan SK (2016) Structural insight into the role of the Ton complex in energy transduction. *Nature* **538**, 60–65.

8 Celia H, Botos I, Ni X, Fox T, De Val N, Lloubes R, Jiang J & Buchanan SK (2019) Cryo-EM structure of the bacterial Ton motor subcomplex ExbB-ExbD provides information on structure and stoichiometry. *Commun Biol* **2**, 358.

9 Celia H, Noinaj N & Buchanan SK (2020) Structure and Stoichiometry of the Ton Molecular Motor. *Int J Mol Sci* **21**.

10 Ratliff AC, Buchanan SK & Celia H (2021) Ton motor complexes. *Curr Opin Struct Biol* **67**, 95–100.

11 Schalk IJ & Guillon L (2013) Fate of ferrisiderophores after import across bacterial outer membranes: different iron release strategies are observed in the cytoplasm or periplasm depending on the siderophore pathways. *Amino Acids* **44**, 1267–1277.

12 Schalk IJ, Rigouin C & Godet J (2020) An overview of siderophore biosynthesis among fluorescent Pseudomonads and new insights into their complex cellular organization. *Environ Microbiol* **22**, 1447–1466.

13 Llamas MA, Mooij MJ, Sparrius M, Vandenbroucke-Grauls CM, Ratledge C & Bitter W (2008) Characterization of five novel *Pseudomonas aeruginosa* cell-surface signalling systems. *Mol Microbiol* **67**, 458–72.

14 Ghysels B, Ochsner U, Mollman U, Heinisch L, Vasil M, Cornelis P & Matthijs S (2005) The *Pseudomonas aeruginosa pirA* gene encodes a second receptor for ferrienterobactin and synthetic catecholate analogues. *FEMS Microbiol Lett* **246**, 167–74.

15 Moynié L, Milenkovic S, Mislin GLA, Gasser V, Malloci G, Baco E, McCaughan RP, Page MGP, Schalk IJ, Ceccarelli M & Naismith JH (2019) The complex of ferric-enterobactin with its transporter from *Pseudomonas aeruginosa* suggests a two-site model. *Nat Commun* **10**, 3673.

16 Elias S, Degtyar E & Banin E (2011) FvbA is required for vibriobactin utilization in *Pseudomonas aeruginosa*. *Microbiology* **157**, 2172–80.

17 Normant V, Josts I, Kuhn L, Perraud Q, Fritsch S, Hammann P, Mislin GLA, Tidow H & Schalk IJ (2020) Nocardamine-Dependent Iron Uptake in *Pseudomonas aeruginosa*: Exclusive Involvement of the FoxA Outer Membrane Transporter. *ACS Chem Biol* **15**, 2741–2751.

18 Llamas MA, Sparrius M, Kloet R, Jimenez CR, Vandenbroucke-Grauls C & Bitter W (2006) The heterologous siderophores ferrioxamine B and ferrichrome activate signaling pathways in *Pseudomonas aeruginosa*. *J Bacteriol* **188**, 1882–91.

19 Hannauer M, Barda Y, Mislin GL, Shanzer A & Schalk IJ (2010) The ferrichrome uptake pathway in *Pseudomonas aeruginosa* involves an iron release mechanism with acylation of the siderophore and a recycling of the modified desferrichrome. *J Bacteriol* **192**, 1212–20.

20 Chan DCK & Burrows LL (2023) *Pseudomonas aeruginosa* FpvB Is a High-Affinity Transporter for Xenosiderophores Ferrichrome and Ferrioxamine B. *mBio* **14**, e0314922.

21 Marshall B, Stintzi A, Gilmour C, Meyer J-M & Poole K (2009) Citrate-mediated iron uptake in *Pseudomonas aeruginosa*: involvement of the citrate-inducible FecA receptor and the FeoB ferrous iron transporter. *Microbiology (Reading, Engl)* **155**, 305–315.

22 Perraud Q, Kuhn L, Fritsch S, Graulier G, Gasser V, Normant V, Hammann P & Schalk IJ (2022) Opportunistic use of catecholamine neurotransmitters as siderophores to access iron by *Pseudomonas aeruginosa*. *Environ Microbiol*. **24**, 878-893

23 Luscher A, Gasser V, Bumann D, Mislin GLA, Schalk IJ & Köhler T (2022) Plant-Derived Catechols Are Substrates of TonB-Dependent Transporters and Sensitize *Pseudomonas aeruginosa* to Siderophore-Drug Conjugates. *mBio*, e0149822.

24 Alejandre-Castañeda V, Patiño-Medina JA, Valle-Maldonado MI, Nuñez-Anita RE, Santoyo G, Castro-Cerritos KV, Ortiz-Alvarado R, Corrales-Escobosa AR, Ramírez-Díaz MI, Gutiérrez-Corona JF, López-Torres A, Garre V & Meza-Carmen V (2022) Secretion of the siderophore rhizoferrin is regulated by the cAMP-PKA pathway and is involved in the virulence of *Mucor lusitanicus*. *Sci Rep* **12**, 10649.

25 Madsen JLH, Johnstone TC & Nolan EM (2015) Chemical Synthesis of Staphyloferrin B Affords Insight into the Molecular Structure, Iron Chelation, and Biological Activity of a Polycarboxylate Siderophore Deployed by the Human Pathogen *Staphylococcus aureus*. *J Am Chem Soc* **137**, 9117–9127.

26 Johnson JR, Moseley SL, Roberts PL & Stamm WE (1988) Aerobactin and other virulence factor genes among strains of *Escherichia coli* causing urosepsis: association with patient characteristics. *Infect Immun* **56**, 405–412.

27 le Roy D, Expert D, Razafindratsita A, Deroussent A, Cosme J, Bohuon C & Andremont A (1992) Activity and specificity of a mouse monoclonal antibody to ferric aerobactin. *Infect Immun* **60**, 768–772.

28 Akers HA (1983) Isolation of the siderophore schizokinen from soil of rice fields. *Appl Environ Microbiol* **45**, 1704–1706.

29 Storey EP, Boghozian R, Little JL, Lowman DW & Chakraborty R (2006) Characterization of "Schizokinen"; a dihydroxamate-type siderophore produced by *Rhizobium leguminosarum* IARI 917. *Biometals* **19**, 637–649.

30 Cuiv PO, Clarke P & O'Connell M (2006) Identification and characterization of an iron-regulated gene, *chtA*, required for the utilization of the xenosiderophores aerobactin, rhizobactin 1021 and schizokinen by *Pseudomonas aeruginosa*. *Microbiology* **152**, 945–54.

31 Cooper JD, Hannauer M, Marolda CL, Briere L-AK & Heinrichs DE (2014) Identification of a positively charged platform in *Staphylococcus aureus* HtsA that is essential for ferric staphyloferrin A transport. *Biochemistry* **53**, 5060–5069.

32 Perraud Q, Cantero P, Roche B, Gasser V, Normant VP, Kuhn L, Hammann P, Mislin GLA, Ehret-Sabatier L & Schalk IJ (2020) Phenotypic Adaption of *Pseudomonas aeruginosa* by Hacking Siderophores Produced by Other Microorganisms. *Mol Cell Proteomics* **19**, 589–607.

33 Hoegy F, Lee X, Noël S, Mislin GL, Rognan D, Reimmann C & Schalk IJ (2009) Stereospecificity of the siderophore pyochelin outer membrane transporters in fluorescent Pseudomonads. *J Biol Chem* **284**, 14949–57.

423 34 Hoegy F & Schalk IJ (2014) Monitoring iron uptake by siderophores. *Methods Mol Biol* **1149**, 337–
424 46.
425 35 Bouyssié D, Hesse A-M, Mouton-Barbosa E, Rompais M, Macron C, Carapito C, Gonzalez de Peredo
426 A, Couté Y, Dupierris V, Burel A, Menetrey J-P, Kalaitzakis A, Poisat J, Romdhani A, Burlet-Schiltz O,
427 Cianférani S, Garin J & Bruley C (2020) Proline: an efficient and user-friendly software suite for large-
428 scale proteomics. *Bioinformatics* **36**, 3148–3155.
429 36 Kuhn L, Vincent T, Hammann P & Zuber H (2023) Exploring Protein Interactome Data with IPinquiry:
430 Statistical Analysis and Data Visualization by Spectral Counts. *Methods Mol Biol* **2426**, 243–265.
431 37 Gregori J, Sanchez A & Villanueva J (2019) msmsTests: LC-MS/MS Differential Expression Tests. .
432 38 Vizcaíno JA, Csordas A, del-Toro N, Dianes JA, Griss J, Lavidas I, Mayer G, Perez-Riverol Y, Reisinger
433 F, Ternent T, Xu Q-W, Wang R & Hermjakob H (2016) 2016 update of the PRIDE database and its related
434 tools. *Nucleic Acids Res* **44**, D447-456.
435 39 Gasser V, Baco E, Cunrath O, August PS, Perraud Q, Zill N, Schleberger C, Schmidt A, Paulen A,
436 Bumann D, Mislin GLA & Schalk IJ (2016) Catechol siderophores repress the pyochelin pathway and
437 activate the enterobactin pathway in *Pseudomonas aeruginosa*: an opportunity for siderophore-
438 antibiotic conjugates development. *Environ Microbiol* **18**, 819–832.
439 40 Dean CR, Neshat S & Poole K (1996) PfeR, an enterobactin-responsive activator of ferric
440 enterobactin receptor gene expression in *Pseudomonas aeruginosa*. *J Bacteriol* **178**, 5361–5369.
441 41 Michel L, Gonzalez N, Jagdeep S, Nguyen-Ngoc T & Reimmann C (2005) PchR-box recognition by the
442 AraC-type regulator PchR of *Pseudomonas aeruginosa* requires the siderophore pyochelin as an
443 effector. *Mol Microbiol* **58**, 495–509.
444 42 Perraud Q, Cantero P, Munier M, Hoegy F, Zill N, Gasser V, Mislin GLA, Ehret-Sabatier L & Schalk IJ
445 (2020) Phenotypic Adaptation of *Pseudomonas aeruginosa* in the Presence of Siderophore-Antibiotic
446 Conjugates during Epithelial Cell Infection. *Microorganisms* **8**, 1820

43 Normant V, Kuhn L, Munier M, Hammann P, Mislin GLA & Schalk IJ (2021) How the Presence of Hemin Affects the Expression of the Different Iron Uptake Pathways in *Pseudomonas aeruginosa* Cells. *ACS Infect Dis*. **15**, 2741-2751

44 Fritsch S, Gasser V, Peukert C, Pinkert L, Kuhn L, Perraud Q, Normant V, Brönstrup M & Schalk IJ (2022) Uptake Mechanisms and Regulatory Responses to MECAM- and DOTAM-Based Artificial Siderophores and Their Antibiotic Conjugates in *Pseudomonas aeruginosa*. *ACS Infect Dis* **8**, 1134–1146.

45 Cornelis P & Bodilis J (2009) A survey of TonB-dependent receptors in fluorescent Pseudomonads. *Environ Microbiol Rep* **1**, 256–62.

46 Cunrath O, Geoffroy VA & Schalk IJ (2016) Metallome of *Pseudomonas aeruginosa*: a role for siderophores. *Environ Microbiol* **18**, 3258–3267.

47 Hubert D, Réglier-Poupet H, Sermet-Gaudelus I, Ferroni A, Bourgeois ML, Burgel P-R, Serreau R, Dusser D, Poyart C & Coste J (2013) Association between *Staphylococcus aureus* alone or combined with *Pseudomonas aeruginosa* and the clinical condition of patients with cystic fibrosis. *J Cyst Fibros* **12**, 497–503.

48 Bessa LJ, Fazii P, Di Giulio M & Cellini L (2015) Bacterial isolates from infected wounds and their antibiotic susceptibility pattern: some remarks about wound infection. *Int Wound Jl* **12**, 47–52.

49 Rahim K, Saleha S, Zhu X, Huo L, Basit A & Franco OL (2017) Bacterial Contribution in Chronicity of Wounds. *Microb Ecol* **73**, 710–721.

50 Ibberson CB & Whiteley M (2020) The social life of microbes in chronic infection. *Curr Opin Microbiol* **53**, 44–50.

51 Yung DBY, Sircombe KJ & Pletzer D (2021) Friends or enemies? The complicated relationship between *Pseudomonas aeruginosa* and *Staphylococcus aureus*. *Mol Microbiol***116**, 1–15.

52 Jenul C, Keim KC, Jens JN, Zeiler MJ, Schilcher K, Schurr MJ, Melander C, Phelan VV & Horswill AR (2023) Pyochelin biotransformation by *Staphylococcus aureus* shapes bacterial competition with *Pseudomonas aeruginosa* in polymicrobial infections. *Cell Rep* **42**.

473 53 Michel L, Bachelard A & Reimmann C (2007) Ferripyochelin uptake genes are involved in pyochelin-
474 mediated signalling in *Pseudomonas aeruginosa*. *Microbiology (Reading, England)* **153**, 1508–18.
475 54 Cunrath O, Graulier G, Carballido-Lopez A, Pérard J, Forster A, Geoffroy VA, Saint Auguste P,
476 Bumann D, Mislin GLA, Michaud-Soret I, Schalk IJ & Fechter P (2020) The pathogen *Pseudomonas*
477 *aeruginosa* optimizes the production of the siderophore pyochelin upon environmental challenges.
478 *Metallomics* **12**, 2108–2120.
479
480
481

LEGENDS

Figure 1. Chemical structure of rhizoferrin (RHIZOF), staphyloferrin A (STAPH A), aerobactin (AERO), *arthrobactin (ARTHRO) and* schizokinen (SCHIZO).

Figure 2. ^{55}Fe uptake by P. aeruginosa strains mediated by RHIZOF, STAPH A, AERO, ARTHRO and SCHIZO. P. aeruginosa ΔpvdFΔpchA cells were grown in iron-restricted CAA medium in the presence of 10 µM RHIZOF, STAPH A, AERO, ARTHRO, or SCHIZO, to induce expression of the corresponding uptake pathway. Afterwards, bacteria were incubated with 500 nM RHIZOF-^{55}Fe, STAPH A-^{55}Fe, AERO-^{55}Fe, ARTHRO-^{55}Fe, or SCHIZO-^{55}Fe. The amount of ^{55}Fe taken up by the bacteria was measured as a function of time. As a control, the experiment was repeated in the presence of the protonophore CCCP (200 µM). The experiment was repeated with the corresponding ΔchtA and ΔactA deletion mutants of ΔpvdFΔpchA. Error bars were calculated from three independent biological replicates.

Figure 3. Growth of Δ*pvdF*Δ*pchA P. aeruginosa* mutants in the presence of RHIZOF or STAPH A. Δ*pvdF*Δ*pchA* and its corresponding Δ*chtA* and Δ*actA* deletion mutants were grown in CAA medium in the presence (growth kinetics in orange) or presence (kinetics in blue) of 10 µM RHIZOF or STAPH A. Growth was followed by monitoring the optical density at 600 nm. Error bars were calculated from three independent biological replicates.

Figure 4. Growth of ΔpvdFΔpchA P. aeruginosa mutants in the presence of AERO, ARTHRO or SCHIZO. The pyoverdine and pyochelin-deficient strain of P. aeruginosa (ΔpvdFΔpchA) and its corresponding ΔactA and ΔchtA deletion mutants were used. Strains were grown in CAA medium in the presence (growth kinetics in orange) or absence (kinetics in blue) of 10 µM AERO, ARTHRO or SCHIZO. Growth was followed by monitoring the optical density at 600 nm. Error bars were calculated from three independent biological replicates.

508 **Scheme 1. Iron acquisition by the xenosiderophores RHIZOF, STAPH A, AERO, ARTHRO and SCHIZO,**

509 **in *P. aeruginosa*.** For more details see the text.

510

511

512

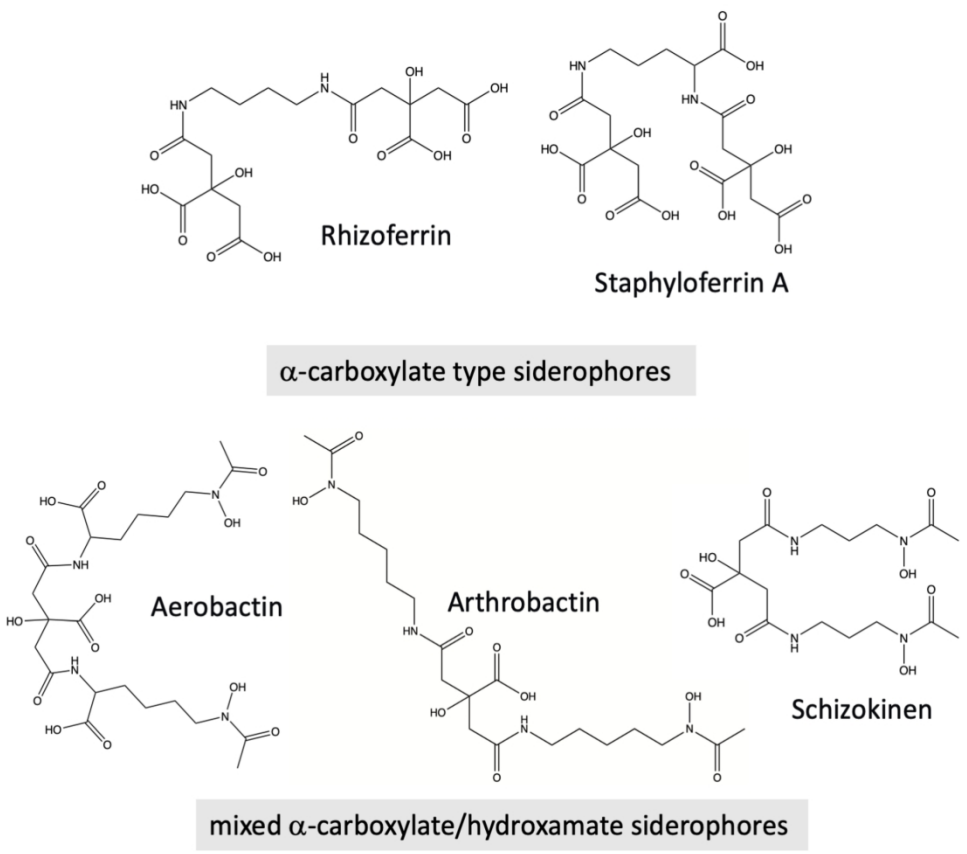

Figure 1. Chemical structure of rhizoferrin (RHIZOF), staphyloferrin A (STAPH A), aerobactin (AERO), arthrobactin (ARTHRO) and schizokinen (SCHIZO).

89x77mm (600 x 600 DPI)

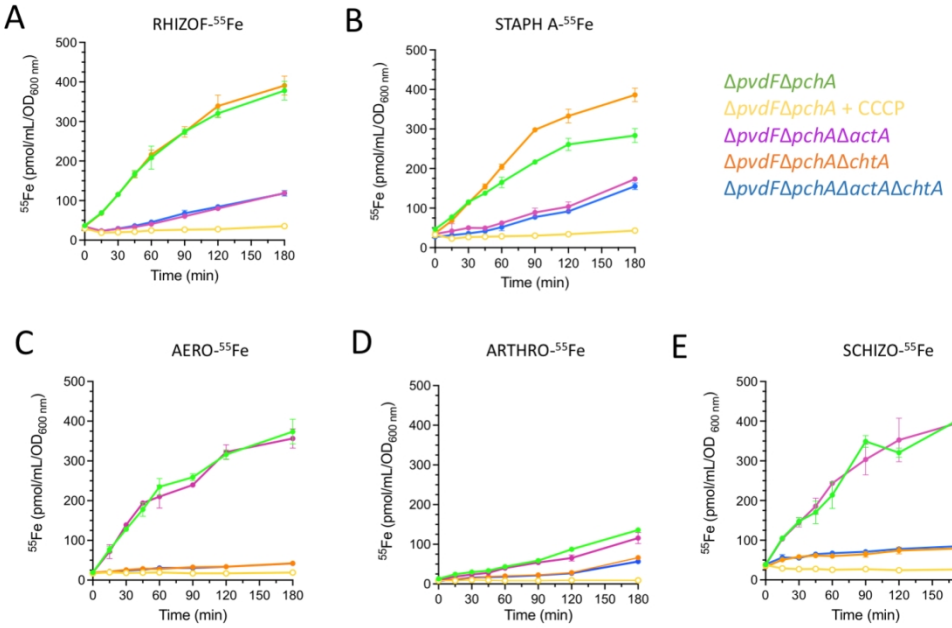

Figure 2. ^{55}Fe uptake by *P. aeruginosa* strains mediated by RHIZOF, STAPH A, AERO, ARTHRO and SCHIZO. *P. aeruginosa* Δ*pvdF*Δ*pchA* cells were grown in iron-restricted CAA medium in the presence of 10 µM RHIZOF, STAPH A, AERO, ARTHRO, or SCHIZO, to induce expression of the corresponding uptake pathway. Afterwards, bacteria were incubated with 500 nM RHIZOF-^{55}Fe, STAPH A-^{55}Fe, AERO-^{55}Fe, ARTHRO-^{55}Fe, or SCHIZO-^{55}Fe. The amount of ^{55}Fe taken up by the bacteria was measured as a function of time. As a control, the experiment was repeated in the presence of the protonophore CCCP (200 µM). The experiment was repeated with the corresponding Δ*chtA* and Δ*actA* deletion mutants of Δ*pvdF*Δ*pchA*. Error bars were calculated from three independent biological replicates.

159x104mm (600 x 600 DPI)

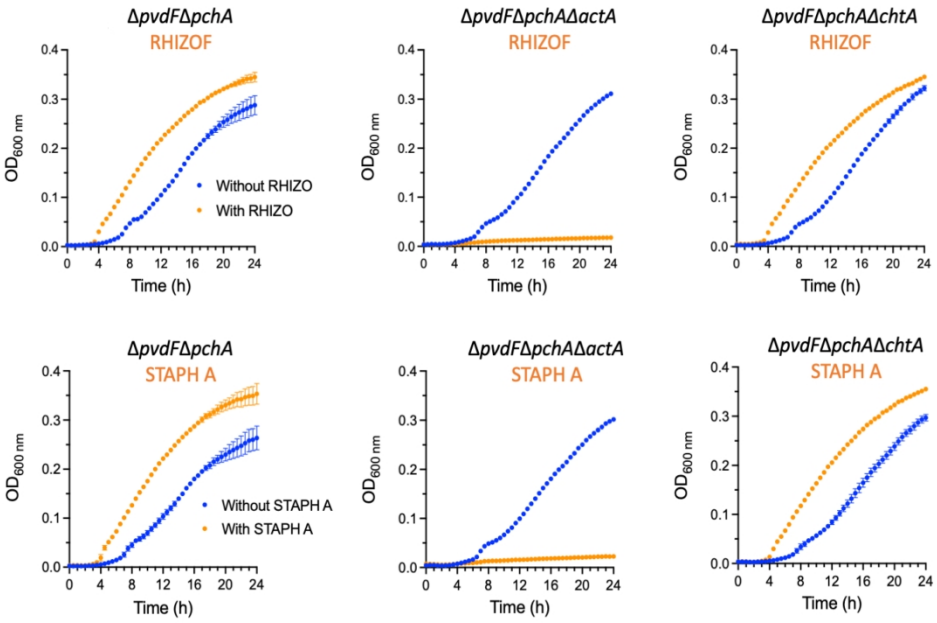

Caption : Figure 3. Growth of ΔpvdFΔpchA P. aeruginosa mutants in the presence of RHIZOF or STAPH A. ΔpvdFΔpchA and its corresponding ΔchtA and ΔactA deletion mutants were grown in CAA medium in the presence (growth kinetics in orange) or presence (kinetics in blue) of 10 µM RHIZOF or STAPH A. Growth was followed by monitoring the optical density at 600 nm. Error bars were calculated from three independent biological replicates.

159x114mm (600 x 600 DPI)

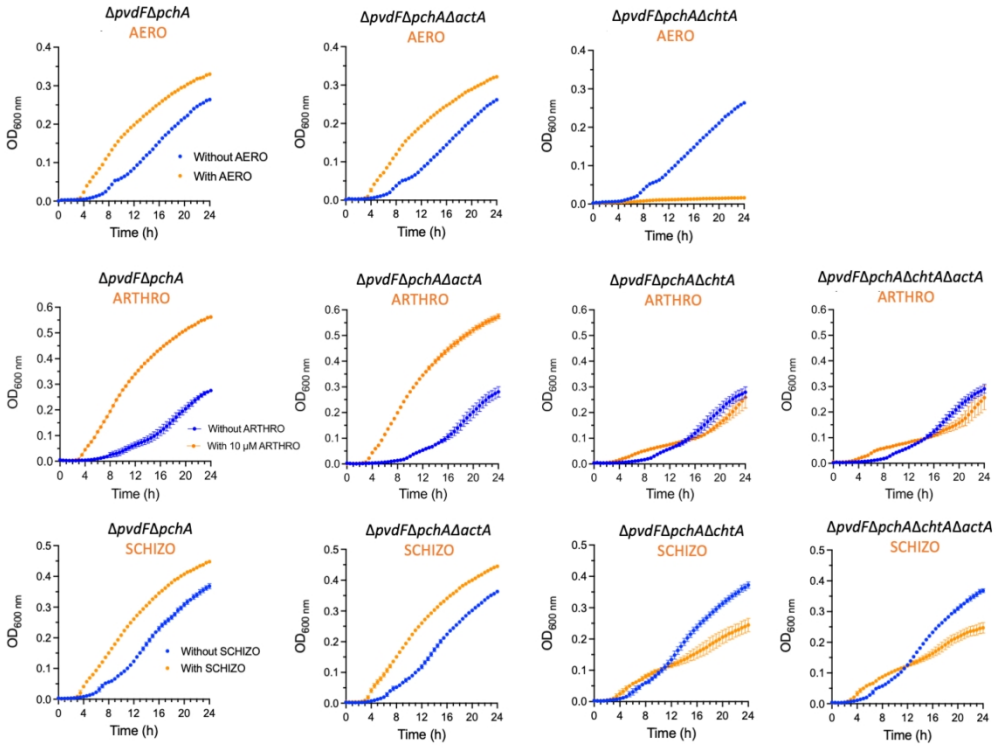

Figure 4. Growth of Δ*pvdF*Δ*pchA P. aeruginosa* mutants in the presence of AERO, ARTHRO or SCHIZO. The pyoverdine and pyochelin-deficient strain of *P. aeruginosa* (Δ*pvdF*Δ*pchA*) and its corresponding Δ*actA* and Δ*chtA* deletion mutants were used. Strains were grown in CAA medium in the presence (growth kinetics in orange) or absence (kinetics in blue) of 10 µM AERO, ARTHRO or SCHIZO. Growth was followed by monitoring the optical density at 600 nm. Error bars were calculated from three independent biological replicates.

169x129mm (600 x 600 DPI)

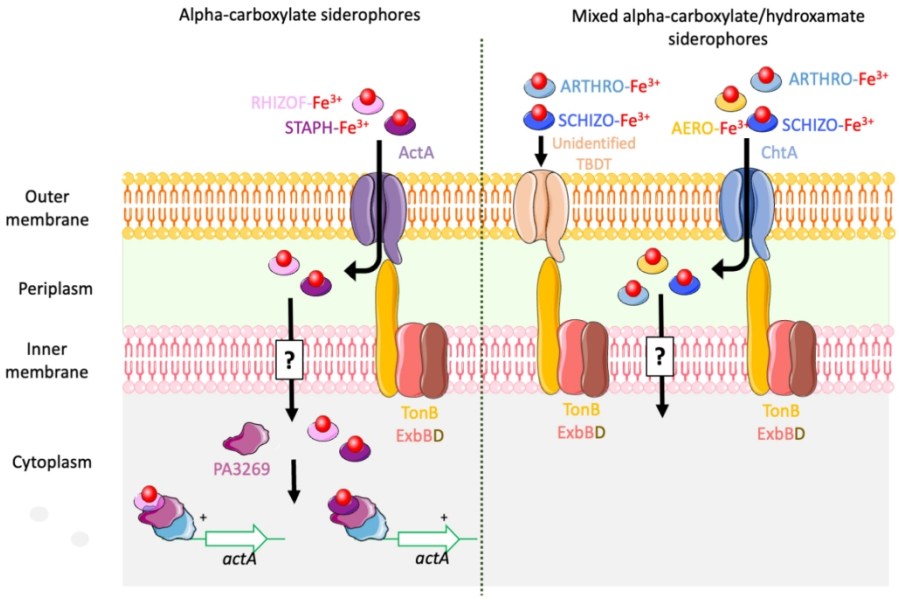

Scheme 1. Iron acquisition by the xenosiderophores RHIZOF, STAPH A, AERO, ARTHRO and SCHIZO, in *P. aeruginosa*. For more details see the text.

89x54mm (600 x 600 DPI)

SUPPLEMENTAL MATERIAL

Siderophore specifities of ChtA and ActA, two TonB-dependent transporters of *Pseudomonas aeruginosa*

Virginie Will[1,2], Véronique Gasser[1,2], Lauriane Kuhn[3], Sarah Fritsch[1,2], David E. Heinrichs[4] and Isabelle J. Schalk[1,2 *].

Table S1. Strains and plasmids used in this study.

Strains and plasmids	Collection ID	Relevant characteristics	Reference
Pseudomonas aeruginosa			
Δ*pvdF*Δ*pchA*	PAS283	PAO1; *pvdF* and *pchA* chromosomally deleted	[1]
Δ*pvdF*Δ*pchA*Δ*chtA*	PAS653	PAO1; *pvdF*, *pchA* and *chtA* chromosomally deleted	This study
Δ*pvdF*Δ*pchA*Δ*actA*	PAS635	PAO1; *pvdF*, *pchA,* and *actA* chromosomally deleted	This sudy
Δ*pvdF*Δ*pchA*Δ*actA*Δ*chtA*	PAS655	PAO1; *pvdF*, *pchA, actA* and *chtA* chromosomally deleted	This study
Escherichia coli			
TOP10		F− mcrA Δ(mrr-hsdRMS-mcrBC) ϕ80lacZΔM15 ΔlacX74 nupG recA1 araD139 Δ(ara-leu)7697 galE15 galK16 rpsL(StrR) endA1 λ−	Invitrogen
Plasmids			
pEXG2	pEXG2	allelic exchange vector with pBR origin, gentamicin resistance, sacB	[2]
pEXG2 Δ*chtA*	pSF07	pEXG2 carrying the sequence to delete *chtA*	This study
pEXG2 Δ*actA*	pSF03	pEXG2 carrying the sequence to delete *PA3268* (*actA*)	This study

Table S2. Primers used for the construction of the Δ*pvdF*Δ*pchA*Δ*chtA*, Δ*pvdF*Δ*pchA*Δ*actA*, and Δ*pvdF*Δ*pchA*Δ*actA*Δ*chtA* strains. *actA* = gene *PA3268*.

Oligonucleotides	Gene	Sequence
PA3268stop-550HindIII-F	*actA*	AAAAAAGCTTGGATCGAATACTTCACCGGGC
PA3268stop+117overlap-R	*actA*	GCACGGTCACCGTGGTCGCGTCGAACCTGAAGCTCGGA
PA3268start-97-F	*actA*	CGACCACGGTGACCGTGC
PA3268start-546XbaI-R	*actA*	AAAATCTAGACGTCCACTTGCACCGCCTG
PA4675Start-784 pb EcoRI	*chtA*	AAAAGAATTCAGTAACGCCCCAGACGAATCG
PA4675Start + 18 pb overlap	*chtA*	CAGGCTGTAGGTCCGCCCCCAGGGGAGCCGGGCG
PA4675Stop + 714 pb HindIII	*chtA*	AAAAAAGCTTTCAAACGAGGGGCATGCCATG
PA4675Stop -18 pb	*chtA*	GGGCGGACCTACAGCCTG

Table S3. Primers used in this study for RT-qPCR.

Oligonucleotides	Sequence (5' to 3')
uvrD F	CTACGGTAGCGAGACCTACAACAA
uvrD R	GCGGCTGACGGTATTGGA
rpsL F	TACACCACCACGCCGAAAA
rpsL R	CACCACCGATGTACGAGGAA
fpvA F	AGCCGCCTACCAGGATAAGC
fpvA R	TGCCGTAATAGACGCTGGTTT
fptA F	GCGCCTGGGCTACAAGATC
fptA R	CCGTAGCGGTTGTTCCAGTT
oprC F	GGACGGCTCGCAGTTCAA
oprC R	AGACCTGTGCCTCGACCTTCT
chtA F	AACGAGAAGATGGCCTTCAATC
chtA R	TCTTCACCAGGGCCAGTTTC
actA F	CGTGCTGCTCAAGACCCATT
actA R	CGTAGGCGTCGTAGTAGTGGAA

Table S3. TBDTs present in the *P. aeruginosa* PAO1 genome.

Gene	Name	Ligand	**Regulation**	Reference
PA0151	-	-	Sigma/anti-sigma factors	[3]
PA0192	-	-		[3]
PA0434	-	-		[3]
PA0470	FiuA	Ferrichrome, ferrichrocin, Fusigen, Rhodotorulic acid	Sigma/anti-sigma factors	[4,5]
PA0781	-	-		[3]
PA0931	PirA	Enterobactin, mono catechol	Two component systems	[6,7]
PA1271	BtuB	Cobalamine		[3]
PA1302	HxuA	Haem	Sigma/anti-sigma factors	[8]
PA1322	PfuA	-		[3]
PA1365	-	-	Sigma/anti-sigma factors	[3]
PA1613	-	-		[3]
PA1910	FemA	Mycobactins, carboxymycobactins	Sigma/anti-sigma factors	[9]
PA1922	CirA	-		[3]
PA2057	SppR	-	Sigma/anti-sigma factors	[10]
PA2070	-	-		[3]
PA2089	-	-	Sigma/anti-sigma factors	[3]
PA2289	-	-		[3]
PA2335	OptO	-		[3]
PA2398	FpvA	Pyoverdine	Sigma/anti-sigma factors	[11]
PA2466	FoxA	Ferrioxamine B, Nocardamine	Sigma/anti-sigma factors	[4,12]
PA2590	-	-		[3]
PA2688	PfeA	Enterobactin	Two component systems	[13]
PA2911	-	-		[3]
PA3268	ActA	Rhizoferrin, Staphyloferrin A	AraC regulators	This study
PA3408	HasR	HasAp-haem	Sigma/anti-sigma factors	[14]
PA3790	OprC	Copper		[3]
PA3901	FecA	Citrate	Sigma/anti-sigma factors	[15]
PA4156	FvbA	Vibriobactin		[16]
PA4168	FpvB	Pyoverdine, ferrichrome, ferrioxamine B		[17,18]
PA4221	FptA	Pyochelin	AraC regulators	[19]
PA4514	PiuA	Mono catechol		[7]
PA4675	ChtA	Aerobactin, Arthrobactin Schizokinen		[20] This study
PA4710	PhuR	Haem		[14]
PA4837	CntO	Pseudopaline		[21]
PA4897	OptI	-	Sigma/anti-sigma factors	[3]

TBDT

Protein	RHIZOF		STAPH A		AERO		SCHIZO	
FptA	-0,3	**	-0,3	*	-0,6	***	-0,8	***
FpvA	-0,3	ns	-0,1	ns	-0,2	ns	-0,3	ns
FpvB	0,2	ns	0,2	ns	0,2	ns	0,0	ns
PA4514	-0,7	ns	0,3	ns	-1,2	ns	-2,0	ns
OprC	-5,6	***	-3,1	**	-1,0	ns	-2,5	*
PhuR	0,2	ns	0,2	ns	0,2	ns	0,1	ns
ChtA	4,3	ns	4,2	ns	3,2	ns	5,2	**
FecA	-0,1	ns	1,0	ns	0,5	ns	1,6	ns
HasR	1,5	ns	1,0	ns	1,89	*	0,1	ns
ActA	2,6	ns	3,1	ns	1,87	ns	3,8	ns
PirA	1,6	ns	1,8	ns	0,28	ns	1,5	ns
PA0434	-1,3	ns	-1,1	ns	-0,14	ns	-2,5	ns

-9 0 9

Ferri-pyochelin uptake pathway

Protein	RHIZOF		STAPH A		AERO		SCHIZO	
PchB	-0,5	ns	-0,2	ns	-1,0	***	-1,1	***
PchC	-0,7	**	-0,5	*	-1,3	***	-2,6	***
PchD	-0,4	**	-0,4	**	-0,9	***	-0,9	***
PchR	0,0	ns	0,0	ns	0,2	ns	-0,5	ns
PchE	-1,2	***	-1,0	***	-1,6	***	-1,2	***
PchF	-2,1	***	-1,1	***	-3,8	***	-2,7	***
PchG	-0,4	ns	-0,1	ns	-0,8	***	-0,9	***
PA4223			3,1	ns				
PA4222	1,9	ns	2,6	ns				
FptA	-0,3	**	-0,3	*	-0,6	***	-0,8	***

Ferri-pyoverdine uptake pathway

Protein	RHIZOF		STAPH A		AERO		SCHIZO	
PvdA	-0,2	*	-0,3	***	-0,1	ns	-0,7	***
PvdQ	-0,1	ns	0,0	ns	0,0	ns	0,0	ns
PvdR	0,0	ns	-0,1	ns	0,0	ns	-0,2	ns
PvdP	-0,3	ns			-0,2	ns	-0,1	ns
PvdN	-0,1	ns	-0,1	ns	0,0	ns	-0,3	ns
PvdO	-0,2	ns	-0,2	ns	-0,1	ns	-0,4	*
PvdE			3,8	ns				
FpvA	-0,3	ns	-0,1	ns	-0,2	ns	-0,3	ns
FpvB	0,2	ns	0,2	ns	0,2	ns	0,0	ns
PvdD	-0,9	ns	-0,7	ns	-0,3	ns	0,9	ns
PvdJ	-1,0	**	-1,4	***	-0,4	ns	0,1	ns
PvdI	-0,5	ns	0,0	ns	0,0	ns	0,9	***
FpvH					3,2	ns	1,8	ns
FpvJ	0,2	ns	-0,1	ns	-0,1	ns	-0,3	ns
FpvK	0,1	ns	-0,6	ns	-0,4	ns	-0,1	ns
FpvC	0,1	ns	0,0	ns	0,2	ns	-0,2	ns
FpvD	0,4	ns	0,3	ns	0,4	ns	0,0	ns
FpvF	0,0	ns	0,1	ns	0,0	ns	0,0	ns
PvdH	-0,1	ns	-0,2	ns	-0,1	ns	-0,2	ns
PvdL	-0,1	ns	0,3	ns	0,3	ns	0,8	***
PvdS	-0,7	ns	-3,9	ns	-0,7	ns	-3,9	ns

Figure S1. A. Differential proteomic analyses of *P. aeruginosa* Δ*pvdF*Δ*pchA* grown in the presence of 10 µM SCHIZO, STAPH A, AERO, or RHIZOF. Δ*pvdF*Δ*pchA* strains were grown in CAA medium, with or without 10 µM SCHIZO, STAPH A, AERO, or RHIZOF, for 8 h and differential proteomic expression analyzed. The average values measured in CAA medium without xenosiderophores were plotted against the average values in CAA supplemented with xenosiderophores. **A-C**. Heat maps of the TBDTs showing a change in their expression (**A**), as well as proteins involved in the pyochelin- (**B**) and pyoverdine-dependent (**C**) iron-uptake pathways. In these heat maps, we chose to show proteins for which a change in the level of expression was observed in one of the conditions analyzed: the darker the shade of red, the more the expression of the protein is repressed; the darker the shade of blue, the more the expression of the protein is induced. ns: data not significant; *p < 0.05, **p < 0.01, and ***p < 0.001

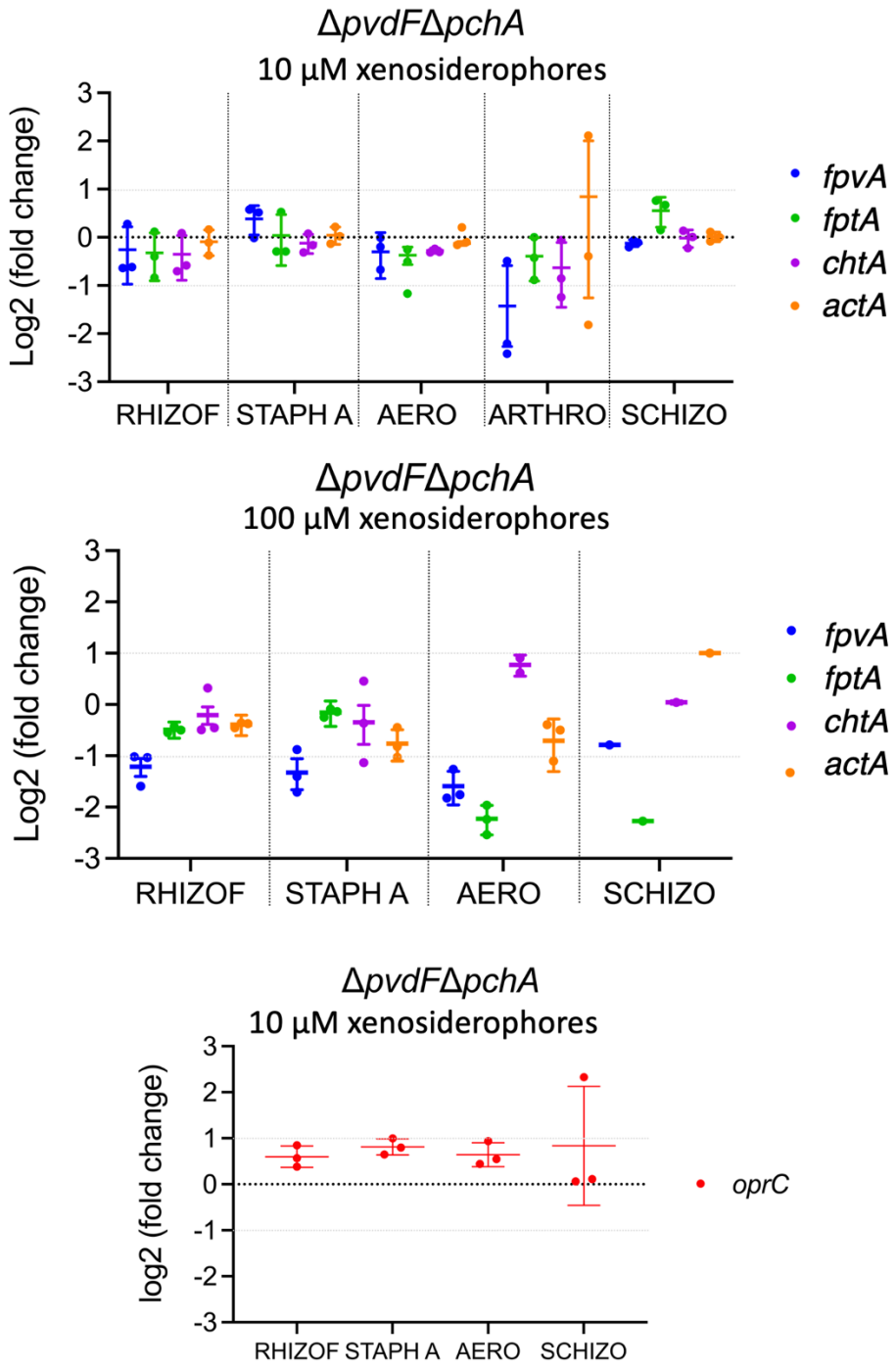

Figure S2. Quantitative real-time PCR on *P. aeruginosa* ΔpvdFΔpchA grown in the presence or absence of SCHIZO, STAPH A, AERO, ARTHRO, or RHIZOF. The Δ*pvdF*Δ*pchA* strain was grown in the presence or absence of 10 µM or 100 µM SCHIZO, STAPH A, AERO, ARTHRO, or RHIZOF. Gene transcription was normalized using the *uvrD* and *rpsL* reference genes. The log2 ratios between the values obtained in the presence of the xenosiderophores and the condition without xenosiderophores are shown. The data show the results of three independent experiments, as well as the mean of the experiment. *fpvA* encodes the TBDT of ferri-pyoverdine, *fptA* the TBDT of ferri-pyochelin, *fecA* the TBDT of ferri-citrate, and *oprC* a TBDT involved in copper uptake.

REFERENCES

1 Gasser V, Baco E, Cunrath O, August PS, Perraud Q, Zill N, Schleberger C, Schmidt A, Paulen A, Bumann D, Mislin GLA & Schalk IJ (2016) Catechol siderophores repress the pyochelin pathway and activate the enterobactin pathway in *Pseudomonas aeruginosa*: an opportunity for siderophore-antibiotic conjugates development. *Environ Microbiol* **18**, 819–832.

2 Rietsch A, Vallet-Gely I, Dove SL & Mekalanos JJ (2005) ExsE, a secreted regulator of type III secretion genes in *Pseudomonas aeruginosa*. *Proc Natl Acad Sci USA* **102**, 8006–8011.

3 Cornelis P & Bodilis J (2009) A survey of TonB-dependent receptors in fluorescent pseudomonads. *Environ Microbiol Rep* **1**, 256–62.

4 Llamas MA, Sparrius M, Kloet R, Jimenez CR, Vandenbroucke-Grauls C & Bitter W (2006) The heterologous siderophores ferrioxamine B and ferrichrome activate signaling pathways in *Pseudomonas aeruginosa*. *J Bacteriol* **188**, 1882–91.

5 Hannauer M, Barda Y, Mislin GL, Shanzer A & Schalk IJ (2010) The ferrichrome uptake pathway in *Pseudomonas aeruginosa* involves an iron release mechanism with acylation of the siderophore and a recycling of the modified desferrichrome. *J Bacteriol* **192**, 1212–20.

6 Ghysels B, Ochsner U, Mollman U, Heinisch L, Vasil M, Cornelis P & Matthijs S (2005) The *Pseudomonas aeruginosa pirA* gene encodes a second receptor for ferrienterobactin and synthetic catecholate analogues. *FEMS Microbiol Lett* **246**, 167–74.

7 Moynié L, Luscher A, Rolo D, Pletzer D, Tortajada A, Weingart H, Braun Y, Page MGP, Naismith JH & Köhler T (2017) Structure and Function of the PiuA and PirA Siderophore-Drug Receptors from *Pseudomonas aeruginosa* and *Acinetobacter baumannii*. *Antimicrob Agents Chemother* **61**.

8 Otero-Asman JR, García-García AI, Civantos C, Quesada JM & Llamas MA (2019) *Pseudomonas aeruginosa* possesses three distinct systems for sensing and using the host molecule haem. *Environ Microbiol*. **21**, 4629-4647.

9 Llamas MA, Mooij MJ, Sparrius M, Vandenbroucke-Grauls CM, Ratledge C & Bitter W (2008) Characterization of five novel *Pseudomonas aeruginosa* cell-surface signalling systems. *Mol Microbiol* **67**, 458–72.

10 Pletzer D, Braun Y & Weingart H (2016) Swarming motility is modulated by expression of the putative xenosiderophore transporter SppR-SppABCD in *Pseudomonas aeruginosa* PA14. *Antonie Van Leeuwenhoek* **109**, 737–753.

11 Poole K, Neshat S & Heinrichs D (1991) Pyoverdine-mediated iron transport in *Pseudomonas aeruginosa:* involvement of a high-molecular-mass outer membrane protein. *FEMS Microbiol Lett* **62**, 1–5.

12 Normant V, Josts I, Kuhn L, Perraud Q, Fritsch S, Hammann P, Mislin GLA, Tidow H & Schalk IJ (2020) Nocardamine-Dependent Iron Uptake in *Pseudomonas aeruginosa*: Exclusive Involvement of the FoxA Outer Membrane Transporter. *ACS Chem Biol* **15**, 2741–2751.

13 Poole K, Young L & Neshat S (1990) Enterobactin-mediated iron transport in *Pseudomonas aeruginosa*. *J Bacteriol* **172**, 6991–6.

14 Smith AD & Wilks A (2015) Differential contributions of the outer membrane receptors PhuR and HasR to heme acquisition in *Pseudomonas aeruginosa*. *J Biol Chem* **290**, 7756–7766.

15 Marshall B, Stintzi A, Gilmour C, Meyer J-M & Poole K (2009) Citrate-mediated iron uptake in *Pseudomonas aeruginosa*: involvement of the citrate-inducible FecA receptor and the FeoB ferrous iron transporter. *Microbiology (Reading, Engl)* **155**, 305–315.

16 Elias S, Degtyar E & Banin E (2011) FvbA is required for vibriobactin utilization in *Pseudomonas aeruginosa*. *Microbiology* **157**, 2172–80.

17 Ghysels B, Dieu BT, Beatson SA, Pirnay JP, Ochsner UA, Vasil ML & Cornelis P (2004) FpvB, an alternative type I ferripyoverdine receptor of *Pseudomonas aeruginosa. Microbiology* **150**, 1671–80.

18 Chan DCK & Burrows LL (2023) *Pseudomonas aeruginosa* FpvB Is a High-Affinity Transporter for Xenosiderophores Ferrichrome and Ferrioxamine B. *mBio* **14**, e0314922.

19 Ankenbauer RG & Quan HN (1994) FptA, the Fe(III)-pyochelin receptor of *Pseudomonas aeruginosa*: a phenolate siderophore receptor homologous to hydroxamate siderophore receptors. *J Bacteriol* **176**, 307–19.

20 Cuiv PO, Clarke P & O'Connell M (2006) Identification and characterization of an iron-regulated gene, *chtA*, required for the utilization of the xenosiderophores aerobactin, rhizobactin 1021 and schizokinen by *Pseudomonas aeruginosa*. *Microbiology* **152**, 945–54.

21 Lhospice S, Gomez NO, Ouerdane L, Brutesco C, Ghssein G, Hajjar C, Liratni A, Wang S, Richaud P, Bleves S, Ball G, Borezée-Durant E, Lobinski R, Pignol D, Arnoux P & Voulhoux R (2017) *Pseudomonas aeruginosa* zinc uptake in chelating environment is primarily mediated by the metallophore pseudopaline. *Sci Rep* **7**, 17132.

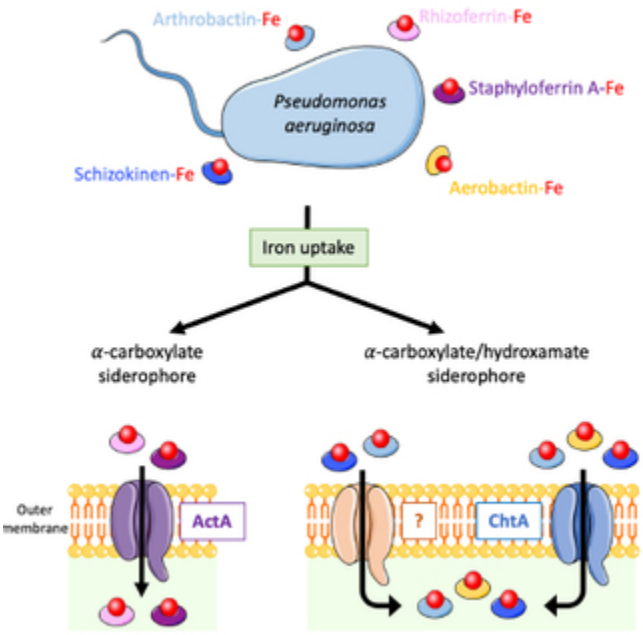

13x13mm (600 x 600 DPI)

Iron is a key nutrient for the growth of almost all bacteria. The pathogen *Pseudomonas aeruginosa* is able to express at least 15 different iron acquisition pathways, each involving a specific outer membrane transporter. Most of these iron uptake pathways relay on small iron chelators (siderophores) produced by other microorganisms. We identified the outer membrane transporters involved in the uptake of iron via two α-carboxylate siderophores and three mixed α-carboxylate/hydroxamate siderophores.